

Amination of Aryl Halides: Quantitative Assessment of Stoichiometric and Catalytic Kinetic Studies

Robert B. Jordan

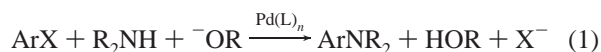
Department of Chemistry, University of Alberta, Edmonton, Alberta, Canada T6G 2G2

Received April 2, 2007

The results of several kinetic studies of the oxidative addition of aryl halides (ArX) to several PdL₂ catalysts have been analyzed to obtain quantitative information on the values of the kinetic parameters. The latter are found to be consistent with reactivity patterns observed for analogous reactions of other Pd(0) systems. These results are applied to several types of kinetic studies of the amination of aryl halides with Pd(0) catalysts. The analysis uses numerical integration of the rate equations after appropriate steady-state assumptions. It is found that in two cases the reaction rate under catalytic conditions is reasonably consistent with rate-limiting oxidative addition. However, in two cases the catalytic rate is either faster or slower than predicted if oxidative addition is rate-limiting. In addition, one example shows a kinetic influence of complexation of Pd(II) by the amine, while for another reductive elimination of the product is rate-limiting.

Introduction

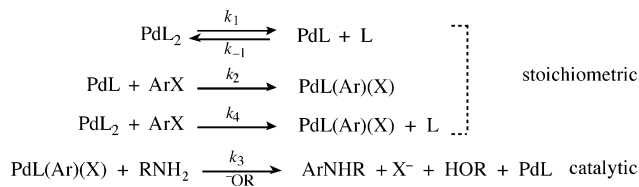
Cross-coupling reactions catalyzed by Pd(0) species are increasingly important for the formation of C–Y bonds, especially for Y = C, O, and N. The area has been the subject of several recent reviews.¹ The overall reaction for C–N bond formation by amination of an aryl halide is shown in reaction 1. There have been several kinetic studies of this reaction, and



much of this work has been discussed and updated in a recent report from three groups that have been major contributors to the area.² The reaction generally is believed to involve oxidative addition of ArX to a Pd(0) complex to give a Pd(Ar)(X) species. This is followed by steps that generally are not rate-controlling. The essential steps are coordination of the amine and its deprotonation by ⁻OR, followed by reductive elimination of the ArNR₂ product and liberation of the catalyst.

Many of the kinetic studies have been done under stoichiometric conditions, in which only ArX and the catalyst are present, because it is believed that this is the rate-controlling step. These studies have provided rate laws for the oxidative addition. Under full catalytic conditions, it has been observed that the rate is independent of the concentration of alkoxide, and the latest studies^{2,3} indicate that the rate is independent of the type and concentration of amine, except for a possible very minor contribution at quite high amine concentrations. A generic set of reactions that can be used to describe the kinetics under stoichiometric and catalytic conditions is shown in Scheme 1. In a recent stoichiometric study³ of the oxidative addition to Pd(BINAP)₂, the *k*₁ pathway was elaborated by including a rapid-equilibrium formation of a monodentate BINAP species that underwent loss of BINAP or oxidative addition by the *k*₄

Scheme 1



pathway. From the point of view of the kinetic analysis, this only adds an unknown equilibrium constant factor to *k*₁ and *k*₄ in the kinetic expressions and has been omitted here for generality and simplicity. The monodentate species also was omitted in the essentially simultaneous, collaborative paper² on the catalytic system from some of the same authors. It should be noted that a more recent report⁴ from one of the major contributors seems to have questioned at least the generality of this mechanism.

The focus of this work is results from several studies with preformed Pd(BINAP)₂ as the catalyst and a more limited study⁵ with a Pd(NHC)₂ catalyst, where NHC is an N-heterocyclic carbene. A remarkable feature of the mechanistic discussion with Pd(BINAP)₂ is that it relies heavily on the qualitative kinetic behavior, and numerical values of the kinetic parameters are rarely given. The kinetic analysis of the Pd(NHC)₂ system was known to be somewhat approximate. The purpose of the present analysis is to determine the kinetic parameters defined by Scheme 1 under stoichiometric conditions and to determine whether these parameters are consistent with the common assumption that oxidative addition is the rate-controlling step under catalytic conditions.

Results

The kinetic parameters presented here have been obtained by least-squares analysis of data extracted from published graphs

(1) Zeni, G.; Larock, R. C. *Chem. Rev.* **2006**, *106*, 4644; Hartwig, J. F. *Synlett* **2006**, 1283; Corbet, J.-P.; Mignani, G. *Chem. Rev.* **2006**, *106*, 2651; Schlummer, B.; Scholz, U. *Adv. Synth. Catal.* **2004**, *346*, 1599.

(2) Shekhar, S.; Ryberg, P.; Hartwig, J. F.; Mathew, J. S.; Blackmond, D. G.; Strieter, E. R.; Buchwald, S. L. *J. Am. Chem. Soc.* **2006**, *128*, 3584.

(3) Shekhar, S.; Ryberg, P.; Hartwig, J. F. *Org. Lett.* **2006**, *8*, 851.

(4) Mathew, J. S.; Klussmann, M.; Iwamura, H.; Valera, F.; Futran, A.; Emanuelsson, E. A. C.; Blackmond, D. G. *J. Org. Chem.* **2006**, *71*, 4711.

(5) Lewis, A. K. K.; Caddick, S.; Cloke, F. G. N.; Billingham, N. C.; Hitchcock, P. B.; Leonard, J. *J. Am. Chem. Soc.* **2003**, *125*, 10066.

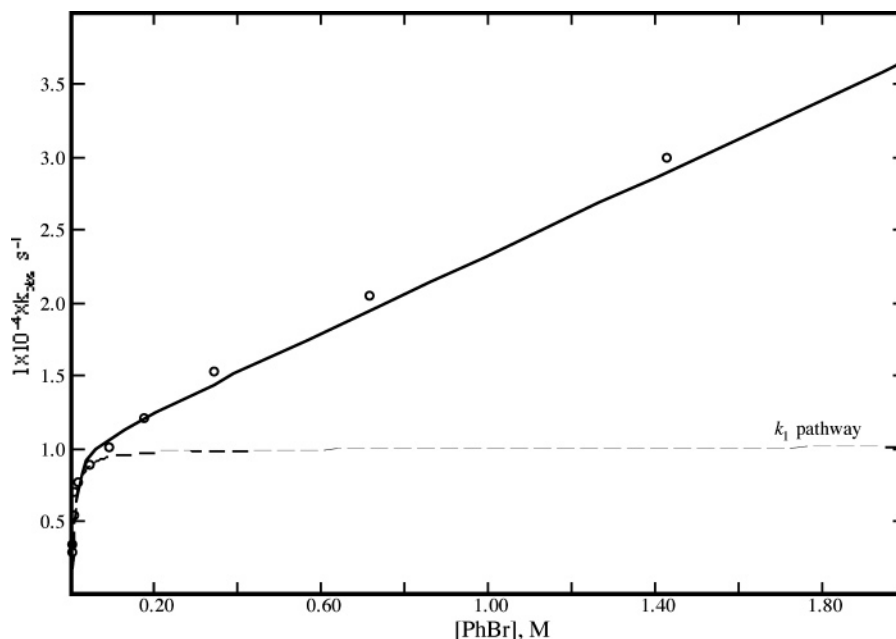


Figure 1. Variation of k_{obsd} with $[\text{PhBr}]$ for the oxidative addition of PhBr to $\text{Pd}(\text{BINAP})_2$ at 45 °C with $[\text{BINAP}] = 4.11 \text{ mM}$ from ref 3. Calculated curves are based on eq 2 and parameters in Table 1; the contribution of the k_1 pathway is shown by the dashed curve.

Table 1. Summary of Kinetic Parameters for Oxidative Addition of ArX to $\text{Pd}(\text{BINAP})_2$ ^a

ArX	solvent	<i>T</i> , °C	k_1k_2/k_{-1} , ^b M ⁻¹ s ⁻¹	k_1 , ^a s ⁻¹	k_{-1}/k_2 , ^a M	k_4 , ^a M ⁻¹ s ⁻¹		ref
PhO ₃ SCF ₃	benzene	45	1.7×10^{-5}	3.3×10^{-4}	20	1.7×10^{-4}	2.9×10^{-8e}	7
PhI	benzene	40	3.8×10^{-3}	2.1×10^{-4}	0.056	4.4×10^{-4}	7.6×10^{-8e}	7
PhBr	toluene	45	6.7×10^{-6}	1.0×10^{-4}	15	1.3×10^{-4}	5.3×10^{-8e}	3
PhBr	toluene	60	$(7 \times 10^{-5})^c$	$(1 \times 10^{-3})^b$	(15)			3
PhBr	toluene	70	1.5×10^{-4d}					3
3-BrC ₆ H ₄ OMe	toluene	70	2.0×10^{-4}	5.4×10^{-3}	27			3

^a Determined by spectrophotometric monitoring of the disappearance of $\text{Pd}(\text{BINAP})_2$ under stoichiometric conditions, unless otherwise indicated. Values determined by least-squares fitting of data extracted from published graphs. ^b Calculated from k_1 and k_{-1}/k_2 where possible. ^c Estimated from one run with 5.7 mM PhBr, 0.41 mM BINAP, and 34 μM $\text{Pd}(\text{BINAP})_2$ and assuming the value of k_{-1}/k_2 at 45 °C. ^d The range of $[\text{BINAP}]$ variation was insufficient to determine the other parameters. ^e Value assuming this pathway has an inverse dependence on $[\text{BINAP}]$.

or by visual fitting of data from various time variation curves using numerical integration by the fourth-order Runge–Kutta algorithm.

Kinetics with $\text{Pd}(\text{BINAP})_2$ under Stoichiometric Conditions. These studies^{3,6,7} have used mainly spectrophotometry to monitor the disappearance of $\text{Pd}(\text{BINAP})_2$ as it forms $(\text{BINAP})\text{Pd}(\text{Ar})(\text{X})$ in the presence of excess ArX. The rate of oxidative addition of ArX to $\text{Pd}(\text{BINAP})_2$ shows saturation behavior in the concentration of ArX and an inverse dependence on the concentration of BINAP. With $[\text{ArX}] > 0.1 \text{ M}$, several halides show an additional first-order dependence on $[\text{ArX}]$, and this has been attributed to the k_4 pathway in Scheme 1. Representative results³ for reaction with PhBr are shown in Figure 1.

For the stoichiometric conditions of these experiments with $[\text{ArX}] \gg [\text{Pd}]$, a steady-state assumption for $\text{Pd}(\kappa^2\text{-BINAP}) = \text{PdL}$ gives the pseudo-first-order rate constant for the mechanism in Scheme 1 shown in eq 2. This rate law has been used

$$k_{\text{obsd}} = \frac{k_1[\text{ArX}]}{[\text{ArX}] + \frac{k_{-1}}{k_2}[\text{BINAP}]} + k_4[\text{ArX}] \quad (2)$$

(6) Alcazar-Roman, L. M.; Hartwig, J. F.; Rheingold, A. L.; Lable-Sands, L. M.; Guzei, I. A. *J. Am. Chem. Soc.* **2000**, *122*, 4618.

(7) Alcazar-Roman, L. M.; Hartwig, J. F. *Organometallics* **2002**, *21*, 491.

to fit the data to give the calculated curves in Figure 1 and the numerical results in Table 1. Analogous results for other ArX systems and temperatures are also given in Table 1.

An obvious requirement of the mechanism in Scheme 1 is that k_1 should be independent of the nature of the ArX reactant. It was noted in an early study⁶ that the limiting rate constant at 0.1 M bromobenzene (PhBr) was the same as the rate constant at 0.89 M for 2-bromoanisole, 2-bromo-*p*-xylene, and 2-bromotoluene, but subsequent work which revealed the k_4 pathway at high $[\text{ArX}]$ casts doubt on this evidence because the k_4 contribution should make k_{obsd} increase by about a factor of 2 between 0.1 and 0.89 M on the basis of the most recent data³ for PhBr (see Figure 1).

Two years later, results for phenyl trifluoromethanesulfonate (PhOTf), phenyl bromide, and phenyl iodide were reported,⁷ the first two at 45 °C and the third at 40 °C. This work presents a stronger test for the constancy of k_1 because of the much larger change in the reaction center. Unfortunately, the use of different temperatures obfuscates the issue. It should be noted that some care is necessary in the selection of the data for the PhBr and PhOTf systems. Blackmond and co-workers⁴ have noted the inconsistency between earlier^{6,7} and more recent³ studies of PhBr; the more recent results are used here. For PhOTf, the ambiguities do not affect the value of k_1 and change the other parameters by a factor of 2.⁸

Least-squares fitting of the full range of concentrations⁹ to eq 2 yields the parameters in Table 1 for PhOTf, PhI, and PhBr. The values of k_1 at 40–45 °C fall in the narrow range of $(1 - 3.3) \times 10^{-4} \text{ s}^{-1}$ and do not show any systematic temperature dependence between 40 and 45 °C. The value for PhBr in toluene at 45 °C is somewhat less certain because of the difficulty in reading low values of [PhBr] from the published graph. My overall impression is that the values of k_1 are reasonably constant as predicted by the mechanism in Scheme 1.

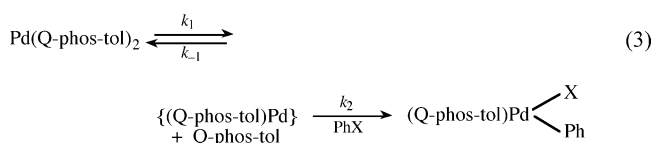
The variation of k_{-1}/k_2 with the nature of X in ArX should show a trend consistent with other studies on the oxidative additions to Pd(0) species. The mechanism suggests that k_{-1} should be independent of the nature of X, but k_2 should be largest for the most reactive ArX. Jutland and co-workers^{10,11} studied the oxidative addition of PhI, PhOTf, and PhBr to Pd(PPh₃)₄ in DMF, and from their data one can estimate relative reactivities of $\sim 1 \times 10^4$, 1.5, and 1.0, respectively. In other words, PhI is by far the most reactive, while PhOTf and PhBr are similar. The values of k_{-1}/k_2 in Table 1 fit the expected trend; PhBr and PhOTf have similar values, while that for PhI is $\sim 3 \times 10^{-3}$ times smaller.

It is also possible to determine whether the relative reactivities of PhBr and 3-bromoanisole with Pd(BINAP)₂ are consistent with previous observations with other phosphine complexes of Pd(0). The stoichiometric study of 3-bromoanisole³ involved variation of [BINAP] between 1.2 and 8.2 mM with [ArBr] = 4.7 mM and showed a concentration dependence consistent with eq 2, except that the k_4 pathway was not apparent because of the low [ArBr]. The [BINAP] dependence³ of the reaction of these two aryl bromides at 70 °C yields values for $k_1 k_2/k_{-1}$ of 1.5×10^{-4} and 2.0×10^{-4} , respectively, as given in Table 1. Several earlier studies^{10,12,13} found that the rates of these types of reactions with a different source of Pd(0) show a reasonable correlation with Hammett's σ substituent constants with $\rho \approx 2$. This predicts that 3-bromoanisole should be ~ 2 times more reactive than PhBr. The results with Pd(BINAP)₂ are reasonably consistent with this prediction, given the differences in the source of Pd(0), temperature, and solvent for the substituent effect studies.

The values of $k_1 k_2/k_{-1}$ for PhBr at different temperatures, given in Table 1, allow one to estimate activation parameters for this parameter. The appropriate plot shown in the Supporting Information is consistent with $\Delta H^\ddagger \approx 28 \text{ kcal mol}^{-1}$ and $\Delta S^\ddagger \approx 5.7 \text{ cal mol}^{-1} \text{ K}^{-1}$.

The discussion thus far suggests a common mechanism for oxidative addition of different ArX to Pd(BINAP)₂. On the other

hand, Barrios-Laneros and Hartwig¹⁴ recently suggested "distinct mechanisms" for the oxidative addition of PhI, PhBr, and PhCl to a bis(phosphine)palladium(0) complex, Pd(Q-phos-tol)₂. The reactions were studied in THF with [PhX] in the rather high range of ~ 0.7 to $\sim 6 \text{ M}$ and [Q-phos-tol] in the range of 0–0.3 M. For PhI at 30 °C, the rate was first-order in [PhI] and independent of [Q-phos-tol], for PhBr at 50 °C, the rate was independent of both [PhBr] and [Q-phos-tol], and for PhCl at 60 °C, the rate had a positive dependence on [PhCl] and an inverse dependence on [Q-phos-tol]. The observations with PhCl were considered to be consistent with a mechanism analogous to the k_1 pathway in Scheme 1, as shown in eq 3. For PhCl, the



data yield $k_1 = 2 \times 10^{-3} \text{ s}^{-1}$ and $k_{-1}/k_2 = 48$ at 60 °C. These agree with the published values of $(2 \pm 0.2) \times 10^{-3} \text{ s}^{-1}$ and between 30 and 50, respectively. The results with PhBr do not require a different mechanism but only that k_{-1}/k_2 is smaller, as expected for the more reactive halide, so that $[\text{PhBr}] \gg (k_{-1}/k_2)[\text{Q-phos-tol}]$. The measured rate constant for PhBr at 60 °C does correspond numerically to the value of k_1 determined with PhCl. Because the rate law for reaction 3 will not reduce to the form observed with PhI, Barrios-Laneros and Hartwig proposed a mechanism involving direct addition of PhI to Pd(Q-phos-tol)₂. This corresponds to k_4 in Scheme 1 if L is a monodentate ligand, and eq 2 would apply. Then, if [PhI] were lower, i.e., $< 0.1 \text{ M}$, PhI might be reacting by the pathway in eq 3 like the others. From the published data and Supporting Information, one can estimate that the rate constants for direct addition of PhI (k_4) and for dissociation of Q-phos-tol (k_1) at 30 °C are $\sim 5 \times 10^{-4} \text{ M}^{-1} \text{ s}^{-1}$ and $6 \times 10^{-5} \text{ s}^{-1}$, respectively. From the previous discussion of trends in values, it seems likely that $k_{-1}/k_2 \ll 1$ for PhI, so that $[\text{PhI}] \gg (k_{-1}/k_2)[\text{Q-phos-tol}]$ if the PhI and phosphine concentrations are similar. Then, for example, if $[\text{PhI}] = 5 \times 10^{-3} \text{ M}$, the direct addition will have $k_{\text{obsd}} = 2.5 \times 10^{-6} \text{ s}^{-1}$, while the pathway in reaction 3 will have $k_{\text{obsd}} = 6 \times 10^{-5} \text{ s}^{-1}$, and the latter will be dominant for millimolar levels of [PhI]. This is consistent with the observations of Amatore and Pflüger¹² on the reaction of PhI with Pd(PPh₃)₄, where concentrations were in the millimolar range. It seems that all of these systems may be described by Scheme 1, but PhI is different from the others in using the k_4 pathway under the high [PhI] used by Barrios-Laneros and Hartwig.

There is ample precedent for the direct or associative pathway for oxidative addition to PdL₂ species, where L is monodentate. It is also known that this pathway is very sensitive to the halide on the electrophile, with the reactivity order $\text{I} \gg \text{Br} \gg \text{Cl}$.¹⁵ Therefore, it is not surprising that Barrios-Laneros and Hartwig observed this pathway with PhI, while PhBr and PhCl go by the k_1 or dissociative pathway. The 4-coordinate Pd(BINAP)₂ seems to be different in that the k_4 values are of the same magnitude for different electrophiles. This could be interpreted to mean that breaking a bond to BINAP is a significant rate-controlling factor for this pathway.

Kinetic evidence for the k_4 pathway with Pd(BINAP)₂ was first presented⁷ for PhBr and PhI and was later confirmed for

(8) For the dependence on [BINAP], the graph gives $1/k_{\text{obsd}}$ in the range of 10–40, but k_{obsd} must be on the order of 10^{-4} , on the basis of the dependence on [PhBr] and the latter results of ref 6. However, when this correction is made, the [BINAP] and [PhBr] variation studies give two distinctly different lines on a plot of $1/k_{\text{obsd}}$ versus [BINAP]/[PhBr]. When the k_4 term is insignificant, eq 2 predicts one line. On the basis of the more recent results, the original [PhBr] dependence is erroneous for some reason; no change in [BINAP] during the [PhBr] variation will make the results internally consistent. There is an analogous problem with the PhOTf data. Either [BINAP] is double the $1.7 \times 10^{-4} \text{ M}$ value given for the [PhOTf] study, or [PhOTf] is double the $2.26 \times 10^{-4} \text{ M}$ value given for the [BINAP] study.

(9) The data have been extracted from published graphs and therefore are not the exact raw data but closely representative of the experimental results.

(10) Jutland, A.; Mosleh, A. *Organometallics* **1995**, *14*, 1810.

(11) Jutland, A.; Egri, S. N.; de Vries, J. G. *Eur. J. Inorg. Chem.* **2002**, 1711.

(12) Amatore, C.; Pflüger, F. *Organometallics* **1990**, *9*, 2276.

(13) Portnoy, M.; Milstein, D. *Organometallics* **1993**, *12*, 1665. The ρ value given here is based on a plot of $\ln(k_Y/k_H)$ vs σ and should be divided by 2.3 to put it on the basis of the normal $\log(k_Y/k_H)$ plot.

(14) Barrios-Laneros, F.; Hartwig, J. F. *J. Am. Chem. Soc.* **2005**, *127*, 6944.

(15) Roland, S.; Mangeney, P.; Jutland, A. *Synlett* **2006**, 3088; Hills, I. D.; Netherton, M. R.; Fu, G. C. *Angew. Chem., Int. Ed.* **2003**, *42*, 5749 and references therein.

PhBr,³ although with somewhat different numerical results. The general observation is that k_{obsd} continues to increase as [PhX] increases well beyond the point where [PhX] \gg (k_{-1}/k_2) -[BINAP]. The original formulation shown in Scheme 1 implied that the rate for this pathway was independent of [BINAP], but this has not been systematically explored. A comparison of information from various sources discussed below suggests that there may be an inverse dependence on [BINAP]. Values of k_4 for both possibilities are given in Table 1. The original report⁷ indicated that there was no k_4 contribution for PhOTf, but the present analysis suggests that it may have a magnitude similar to that of the other systems.¹⁶ The numerical consistency of the two sets of data^{3,7} for PhBr that show this kinetic contribution is improved if this pathway has an inverse dependence on [BINAP]. There also is a study² under catalytic conditions with 2 M PhBr that shows an inverse dependence on [BINAP].

Kinetics with Pd(BINAP)₂ under Catalytic Conditions.

Under these conditions, the concentration of catalyst is assumed to be constant and proportional to the initial concentration of Pd(BINAP)₂. The kinetic results under catalytic conditions were interpreted² by a modified version of Scheme 1, in which the k_4 pathway was ignored. If the latter is retained and a steady-state is assumed for PdL and PdL(Ar)(X), then their concentrations are given by eq 4,

$$[\text{PdL}] = \frac{k_1 + k_4[\text{ArX}]}{k_{-1}[\text{L}]} [\text{PdL}_2]$$

$$[\text{PdL}(\text{Ar})(\text{X})] = \frac{k_1k_2 + k_4(k_{-1}[\text{L}] + k_2[\text{ArX}])}{k_{-1}k_3[\text{L}][\text{RNH}_2]} [\text{ArX}][\text{PdL}_2] \quad (4)$$

as shown in the Supporting Information. If the amine is the deficient reagent, then its rate of disappearance is given by eq 5. A version of this rate law with $k_4 = 0$ was derived previously,²

$$-\frac{d[\text{H}_2\text{NR}]}{dt} = k_3[\text{RNH}_2][\text{PdL}(\text{Ar})(\text{X})] = \frac{k_1 + k_4\left(\frac{k_{-1}}{k_2}[\text{L}] + [\text{ArX}]\right)}{\frac{k_{-1}}{k_2}[\text{L}]} [\text{ArX}][\text{PdL}_2] \quad (5)$$

and that form predicts a simple first-order and inverse dependence on [ArX] and [L], respectively. Notable differences between the stoichiometric rate law in eq 2 and the catalytic one in eq 5 are the absence of the [ArX] term in the denominator and the possible [ArX]² dependence of the k_4 term if [ArX] $>$ $(k_{-1}/k_2)[\text{L}]$.

The reaction for PhBr under catalytic conditions² has been studied at relatively high concentrations of PhBr in the range of 0.1–2.2 M. The kinetic data were determined at 50 °C by NMR monitoring of the deficient reagent, 13 mM hexylamine, with 1.26 mM Pd(BINAP)₂. To determine the dependence of the rate on [BINAP], [BINAP] was varied between 2.3 and 9.2 mM while [PhBr] = 2.0 M was maintained. In the published analysis,² the k_4 pathway was omitted so that eq 5 reduces to a form in which k_{obsd} as defined here¹⁷ should increase linearly with [PhBr]/[BINAP] and have a slope of k_1k_2/k_{-1} . The plot is

(16) Data taken from published graphs were fitted by least-squares to versions of eq 2 with and without the k_4 term. The model with the k_4 term gave a slightly better fit, but both models gave adequate fits. Therefore, the k_4 pathway is neither required nor inconsistent with the data for PhOTf.

shown in Figure 2, where the line drawn has a slope of $\sim 6 \times 10^{-6} \text{ M}^{-1} \text{ s}^{-1}$. The problem is that this value at 50 °C is slightly smaller than that from a stoichiometric study at 45 °C (see Table 1); the activation parameters given above predict a value of $\sim 12 \times 10^{-6} \text{ M}^{-1} \text{ s}^{-1}$ at 50 °C.

No rationale has been offered for the omission of the k_4 pathway, although, as can be seen from Figure 1, it makes a major contribution at [PhBr] = 2.0 M. If the k_4 pathway is included, the catalytic results are in much greater disagreement with the stoichiometric predictions, as can be seen from the dashed curve in Figure 2, calculated from the 45 °C parameters in Table 1. If the problem is not just one of kinetic nonreproducibility, then a possible explanation lies with the small concentration of hexylamine (13 mM) in this catalytic study. This presents a possible constraint on the k_3 step and might mean that Pd(BINAP)(Ar)(Br) might accumulate during the reaction, rather than being a steady-state intermediate.

This possibility was tested by numerical integration of the rate equations without the steady-state assumption for Pd-(BINAP)(Ar)(Br) and with values adjusted to 50 °C of $k_1k_2/k_{-1} = 12 \times 10^{-6}$ and $k_4 = 2 \times 10^{-4}$. A value of $k_3 = 3.0$ reproduces the experimental observations for [PhBr] = 2.0 M and [BINAP] = 2.3 mM and gives a reasonable first-order dependence on [PhBr], but the variation of k_{obsd}^{-1} with [BINAP] shows a substantial intercept at [BINAP] = 0 that is not consistent with the experimental observations.

The following question immediately arises: What is the expected magnitude of k_3 ? This turns out to be more difficult to answer than might be thought. The closest system would seem to be the reaction of Pd(P(*o*-tol)₃)(NH₂Bn)(C₆H₄CMe₃)(Br) with NH₂Bn (benzylamine), which was studied by Zhong and Widenhoefer.¹⁸ The aryl and bromide ligands are *trans* in the reactant, and the reaction proceeds by displacement of the phosphine by the amine so that the relationship to the displacement of Br⁻ from Pd(BINAP)(Ph)(Br) is tenuous at best. Nonetheless, it is interesting to note that the rate constant is only $1.25 \times 10^{-3} \text{ M}^{-1} \text{ s}^{-1}$ in C₆D₆ at 55 °C. It is possible from published information to rather indirectly estimate¹⁹ that k_3 might be $\sim 2 \times 10^5 \text{ M}^{-1} \text{ s}^{-1}$.

If the k_4 pathway really is not operative under catalytic conditions, then a possible explanation is that the product of this reaction is not Pd(BINAP)(Ph)(Br) but some species not in the catalytic cycle. The stoichiometric kinetic study that evaluated k_4 measured the disappearance of Pd(BINAP)₂ but did not identify the product(s). Such a process would remove the source of the catalyst from the system and slow the reaction. This system was modeled with the integrated rate law using the parameters adjusted to 50 °C of $k_1k_2/k_{-1} \approx 12 \times 10^{-6}$ and $k_4 \approx 2 \times 10^{-4}$. It was found that the variation of [amine] with time slows sufficiently only when the curves show substantial

(17) The k_{obsd} values plotted in Figure 10 of ref 2 are zeroth-order rate constants (J. Hartwig, private communication) and contain [Pd]_{tot}. The latter (1.26 mM) has been divided out for the present analysis so that k_{obsd} always represents the same quantity here.

(18) Zhong, H. A.; Widenhoefer, R. A. *Inorg. Chem.* **1997**, *36*, 2610.

(19) This estimate is based on the rate constant for solvolysis of *cis*-Pt-(PEt₃)₂(Ph)(Cl) in ethanol of 0.04 s^{-1} . (Basolo, F.; Chatt, J.; Gray, H. B.; Pearson, R. G.; Shaw, B. L. *J. Chem. Soc.* **1961**, 2207). It is assumed that the conductivity method used by Basolo et al. would measure the solvolysis and not the subsequent isomerization that is observed spectrophotometrically (Kelm, H.; Louw, W. J.; Palmer, D. A. *Inorg. Chem.* **1980**, *19*, 843 and references therein). The rate constant was divided by the solvent molarity (17.2) to obtain a second-order rate constant, multiplied by 10³ to convert from an O- to a N-donor nucleophile, on the basis of η_{Pt} values, and multiplied by the 10⁵ rate difference between analogous Pt complexes of Pd and Pt observed by Basolo et al. to obtain $k_3 \approx 2 \times 10^5 \text{ M}^{-1} \text{ s}^{-1}$.

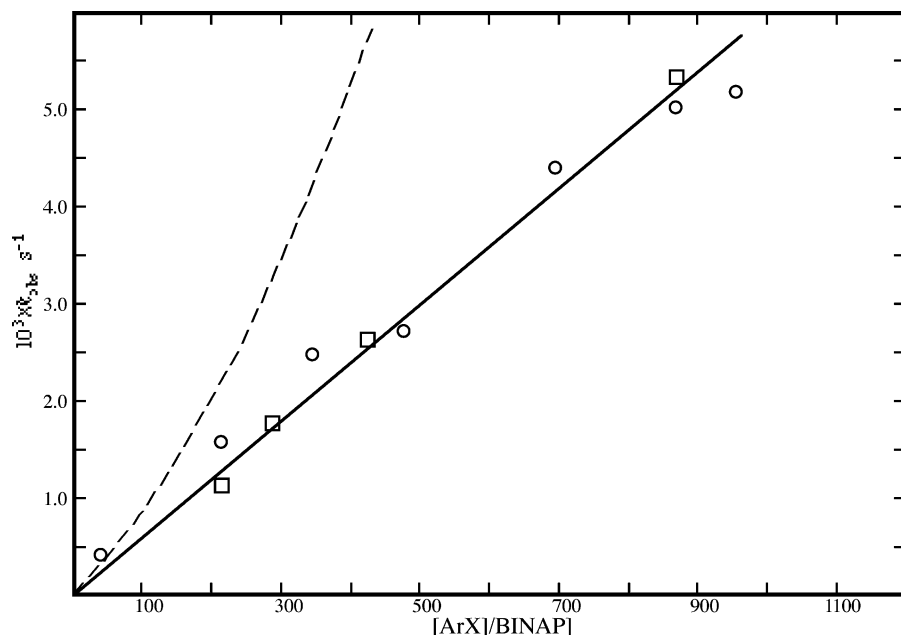


Figure 2. Variation of k_{obsd} with $[\text{PhBr}]/[\text{BINAP}]$ under catalytic conditions at 50 °C with 1.26 mM $\text{Pd}(\text{BINAP})_2$ while loss of *n*-hexylamine is monitored, ref 2: (O) varying $[\text{PhBr}]$ with $[\text{BINAP}] = 2.3$ mM; (□) varying $[\text{BINAP}]$ with $[\text{PhBr}] = 2.0$ M. The dashed curve is calculated from eq 5 using the kinetic parameters at 45 °C in Table 1.

deviation from zeroth-order kinetics that would surely have been noted during the experiments.

There is another set of observations on the reaction of *n*-hexylamine with PhBr under catalytic conditions given in Figure 8a of ref 2. This study differs from the others in that it is a calorimetric reaction progress study at 60 °C using $\text{Pd}(\text{BINAP})_2$ prepared at Imperial College. The initial concentrations were $[\text{PhBr}]_0 = 0.14$ M, $[\text{BINAP}]_0 = 2.0$ mM, and $[\text{n-hexylamine}]_0 = 0.85$ M. The high concentration of the latter should allow the full steady-state rate law to apply, and the rate of disappearance of ArX will be the same as for RNH_2 (eq 5). This predicts that the turnover frequency (TOF) should vary with the fraction of reaction ($\text{FrX} = ([\text{ArX}]_0 - [\text{ArX}])/[\text{ArX}]_0$) as given by eq 6. With the modest $[\text{PhBr}]$ of this experiment,

$$\text{TOF} = \frac{1}{[\text{PdL}_2]} \left(-\frac{d[\text{ArX}]}{dt} \right) = \frac{\frac{k_1 k_2}{k_{-1}} + k_4 \left([\text{BINAP}] + \frac{k_2}{k_{-1}} [\text{ArX}]_0 (1 - \text{FrX}) \right)}{[\text{BINAP}]} [\text{ArX}]_0 (1 - \text{FrX}) \quad (6)$$

one would expect the k_4 pathway to make a minor contribution, in which case eq 6 reduces to eq 7. Therefore, the TOF should vary linearly with Frx, and either the slope or the intercept at

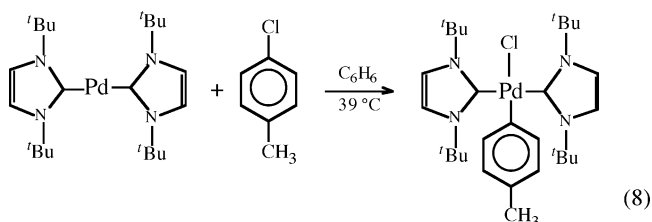
$$\text{TOF} = \frac{k_1 k_2 [\text{ArX}]_0}{k_{-1} [\text{BINAP}]} (1 - \text{FrX}) \quad (7)$$

$\text{Frx} = 0$ can be used to calculate $k_1 k_2 / k_{-1}$. The curves in Figure 3 are actually generated by numerical integration to determine $d[\text{ArX}]/dt$. It is clear for these data that, at $\text{Frx} = 0$, $\text{TOF} \approx 1.2$ min^{-1} , and this yields $k_1 k_2 / k_{-1} = 29 \times 10^{-5} \text{ M}^{-1} \text{ s}^{-1}$. Figure 3 reveals two problems with the observations. The data do not conform very well to the predicted linear variation of TOF with Frx, but more importantly, they yield a value of $k_1 k_2 / k_{-1}$ that is larger than the value at 70 °C from other work³ and is ~6 times larger than the value of $5.2 \times 10^{-5} \text{ M}^{-1} \text{ s}^{-1}$ calculated at 60

°C from the activation parameters under stoichiometric conditions. A calculated curve based on the latter value also is shown in Figure 3.²⁰ If k_4 is adjusted to $\sim 2.5 \times 10^{-2}$ (about 10 times the expected magnitude), then the calculated initial TOF agrees with the data, but the curve is concave, while the data show a convex shape (see Figure 3). There does not seem to be any way to reproduce the data on the basis of reasonable parameters from the stoichiometric study.

In ref 2, there are data for several kinetic runs with 3-bromoanisole at 70 °C under catalytic conditions which indicate that the rate of disappearance of ArX is independent of the nature and concentration (0.45–1 M) of the amine. The results for the coupling of 3-bromoanisole and *N*-methylpiperazine, given in Figure 9 of ref 2, are representative and are shown in Figure 4, along with two calculated curves. The solid curve is calculated by numerical integration using $k_1 k_2 / k_{-1}$ from the stoichiometric study in Table 1. The dashed curve that fits the data is obtained with a 50% higher value of $k_1 k_2 / k_{-1} = 3.0 \times 10^{-4}$ or by including the k_4 pathway with $k_4 = 1.2 \times 10^{-2}$. These data give by far the best agreement between the stoichiometric parameters and the catalytic rate.

Kinetics with $\text{Pd}(\text{NHC})_2$ under Stoichiometric and Catalytic Conditions. This study⁵ differs from those described above both in the catalyst, a palladium(0) *N*-heterocyclic carbene, and the aryl halide, 4-chlorotoluene. Under stoichiometric conditions, the oxidative addition was shown to proceed as shown in reaction 8 with formation of *trans*- $\text{Pd}(\text{NHC})_2(\text{Ar})(\text{Cl})$.



(20) The magnitude for $k_4 \approx 2 \times 10^{-3}$ at 60 °C has been estimated by assuming that k_4 and $k_1 k_2 / k_{-1}$ have the same ΔH^\ddagger .

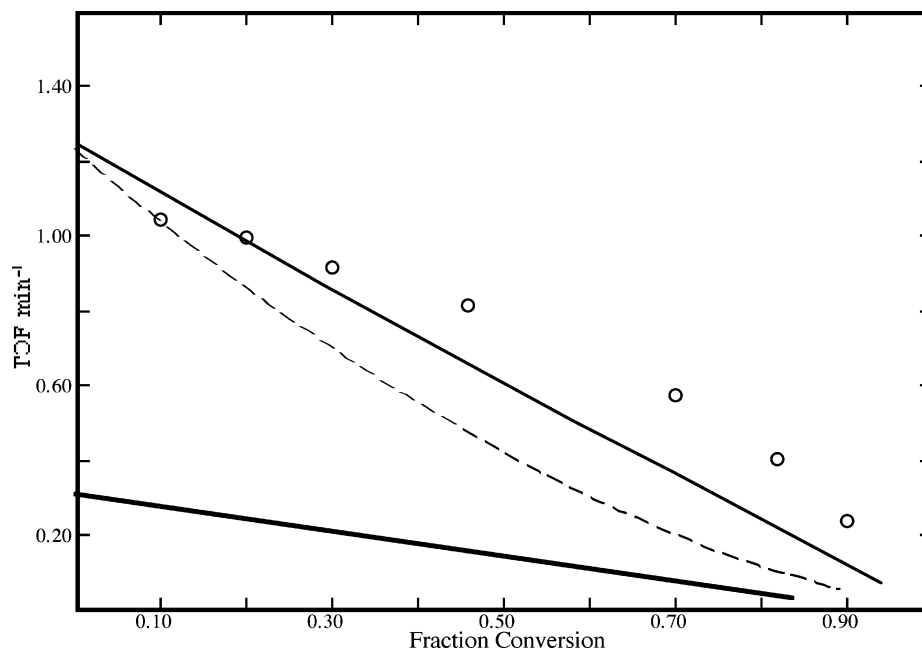


Figure 3. Reaction progress kinetic results under catalytic conditions at 60 °C with 10 mM Pd(BINAP)₂, 2 mM BINAP, ~0.85 M *n*-hexylamine, and 0.14 M initial PhBr from Figure 8a of ref 2. Lines are calculated on the basis of numerical integration with k_1k_2/k_{-1} (M⁻¹ s⁻¹) and k_4 (M⁻¹ s⁻¹) values of 5.2×10^{-5} and 2.0×10^{-3} (dark solid line), 29×10^{-5} and 2.0×10^{-3} (light solid line), and 5.2×10^{-5} and 2.5×10^{-2} (dashed line).

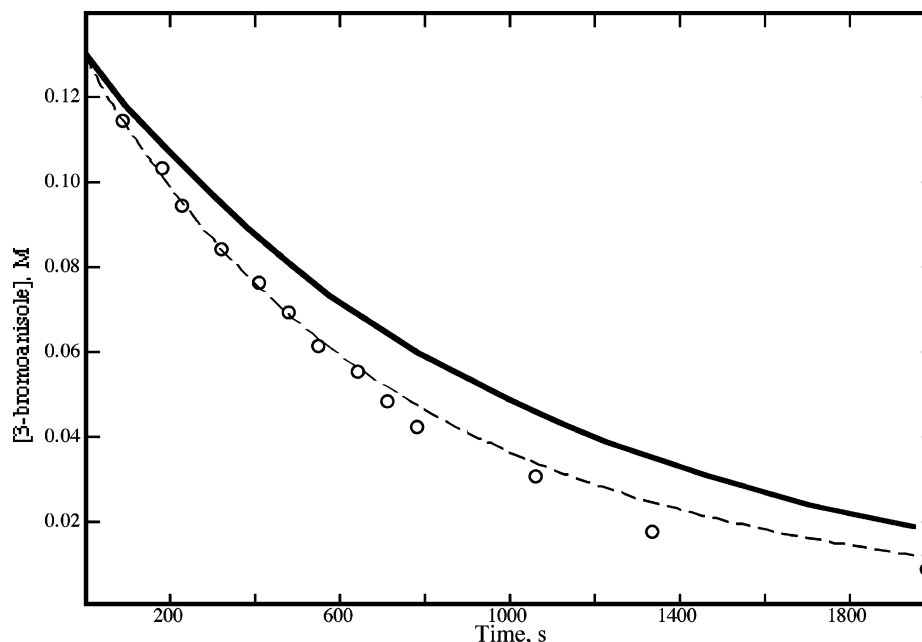


Figure 4. Time dependence of the concentration of 3-bromoanisole during the reaction with *N*-methylpiperazine at 70 °C, catalyzed by 10 mM Pd(BINAP)₂ in the presence of 2 mM BINAP and ~1 M sodium amylate, ref 2. The calculated curves are obtained with $k_1k_2/k_{-1} = 2.0 \times 10^{-4}$ and $k_4 = 0$ (solid line), $k_1k_2/k_{-1} = 2.0 \times 10^{-4}$ and $k_4 = 1.2 \times 10^{-2}$ (dashed line), and $k_1k_2/k_{-1} = 3.0 \times 10^{-4}$ and $k_4 = 0$ (dashed line).

Kinetic studies under stoichiometric conditions at 39 °C in benzene with equal initial concentrations of 0.20 M for Pd(NHC)₂ and ArCl showed increasing inhibition as the concentration of added NHC was changed between 0 and 0.20 M. This is consistent with a mechanism analogous to that in Scheme 1, and the data are consistent with $k_1 = 6.94 \times 10^{-6}$ s⁻¹ and $k_{-1}/k_2 = 20$, as shown by the calculated curves²¹ in Figure 5. There is a problem with a stoichiometric run with [ArX] = 2.0 M and no added NHC that was found to be significantly slower than the run with [ArX] = 0.2 M. The rate law predicts that the rate should be independent of [ArCl] because [ArCl] ≫

[NHC].²² Since the goal here is to determine whether the stoichiometric and catalytic results are consistent, reliance will be placed on the data for [ArCl] = 0.2 M since this was the concentration under catalytic conditions.

In the paper on this system,⁵ values for all of the rate constants are reported, but this results from an incorrect mixing of numbers

(21) Calculated curves are based on rate = $k_1[\text{Pd}(\text{NHC})_2][\text{ArX}]/\{\text{[ArX]} + (k_{-1}/k_2)[\text{NHC}]\}$ using numerical integration to obtain the time dependence of the concentrations.

(22) The run with [ArX] = 2.0 M and no added NHC and the others with [ArX] = 0.2 M and varying added NHC are consistent with $k_1 = 2.8 \times 10^{-6}$ and $k_{-1}/k_2 = 6.6$, as shown in the Supporting Information.

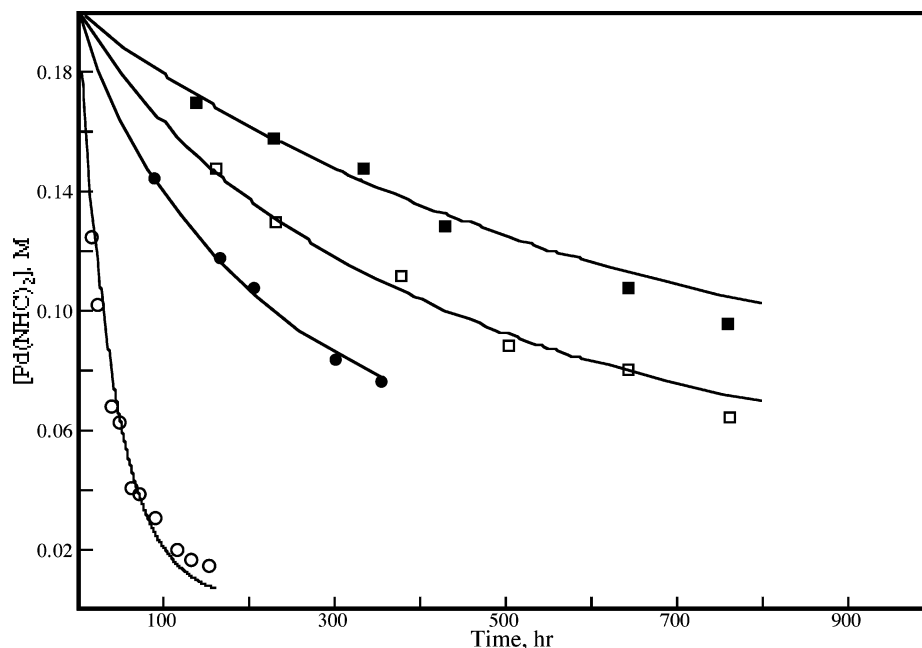


Figure 5. Time dependence of the concentration of the limiting reagent for the reaction of Pd(NHC)₂ with 4-chlorotoluene in benzene at 39 °C, with the following initial conditions: [Pd(NHC)₂] = [ArCl] = 0.2 M, [NHC] = 0 (○), [NHC] = 0.05 M (●), [NHC] = 0.1 M (□), [NHC] = 0.2 M (■).

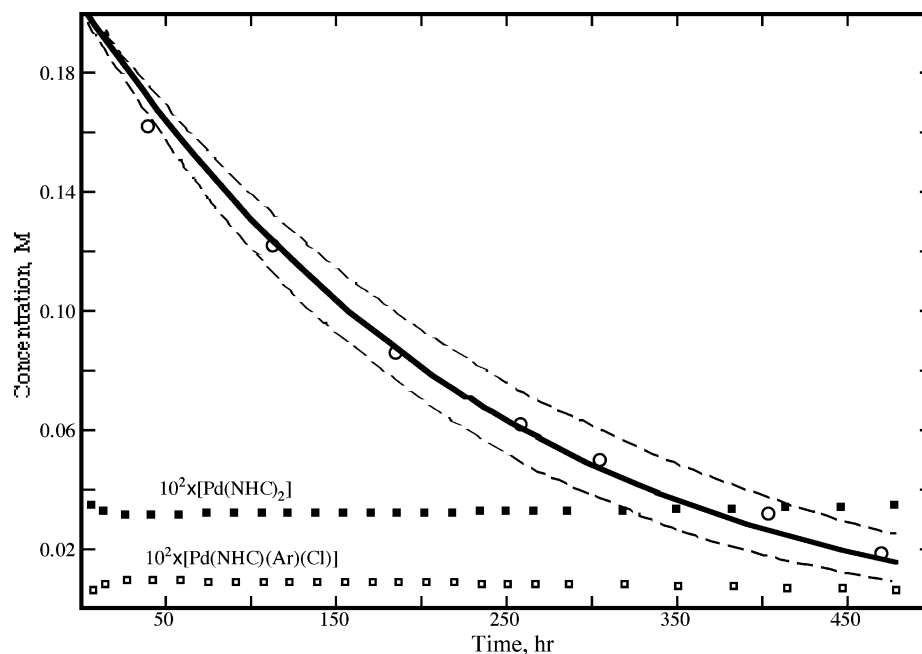


Figure 6. Observed time dependence of the concentrations of 4-chlorotoluene, [ArCl] (○), for the following catalytic conditions: [Pd(NHC)₂] = 4.0×10^{-3} M, [ArCl] = 0.2 M, [NHC] = 0, [morpholine] = 0.23 M, [NaO^tBu] = 0.33 M. The calculations are obtained by numerical integration based on Scheme 1 with kinetic parameters from the stoichiometric studies. The solid curve and concentrations of Pd(NHC)(Ar)(Cl) (□) and Pd(NHC)₂ (■) use $k_3 = 4.3 \text{ M}^{-1} \text{ s}^{-1}$, while the dashed curves assume $\pm 25\%$ larger and smaller k_3 values.

from a steady-state model when [NHC]₀ > 0 with those from a rapid equilibrium assumption when [NHC]₀ = 0. In fact, as shown by the results in Figure 5, only k_1 and k_{-1}/k_2 are needed to describe the observations, and only these parameters can be derived from the results. In the original work, the value of k_1 was obtained from the run with [ArX]₀ = 2.0 M and [NHC]₀ = 0 and k_{-1}/k_2 from the [NHC]₀ variation, and the values do reproduce these runs, but do not fit the run with [ArX]₀ = 0.2 M and [NHC]₀ = 0, as shown in the Supporting Information. The present analysis uses the latter run as a basis for the reason given above.

The catalytic system was studied at 39 °C with initial concentrations of 0.20 M ArCl, 4.0×10^{-3} M Pd(NHC)₂, 0.23 M morpholine, and 0.33 M NaOCEt₃. The rate of disappearance of ArCl was claimed to be first-order in [ArCl] on the basis of a good first-order fit of the variation of [ArCl] with time. However, a more detailed analysis reveals that the system is not so simple, in part because of the similar concentrations of ArCl and amine and also because the rate of formation of the Ar-NRR product affects the observations. The present analysis is based on numerical integration of the system described in Scheme 1.

The results of the analysis are shown in Figure 6, where the calculated curve is produced by the values of k_1 and k_{-1}/k_2 from the stoichiometric studies and $k_3 = 4.3 \text{ M}^{-1} \text{ s}^{-1}$. The sensitivity of the calculated curve to a $\pm 25\%$ change in the value of k_3 is illustrated by the dashed curves in Figure 6. It appears that the stoichiometric kinetic parameters are able to reproduce the observations under catalytic conditions, although the fitting also is sensitive to the value of k_3 . It should be noted that the rather modest magnitude of k_3 seems somewhat unexpected when one realizes that the $\text{Pd}(\text{NHC})(\text{Ar})(\text{Cl})$ species is a three-coordinate $\text{Pd}(\text{II})$ complex and might be expected to be more reactive than the four-coordinate $\text{Pd}(\text{BINAP})(\text{Ar})(\text{Br})$ species discussed in the previous section.

There also is the possibility in this system that $\text{Pd}(\text{NHC})(\text{Ar})(\text{X})$ reacts with the NHC liberated in the k_1 step before undergoing reaction with the amine. This could explain the magnitude of k_3 because amine substitution now would be on four-coordinate $\text{Pd}(\text{NHC})_2(\text{Ar})(\text{X})$. However, reductive elimination would liberate $\text{Pd}(\text{NHC})_2$ rather than the active catalyst $\text{Pd}(\text{NHC})$ and corresponds to the situation where $\text{Pd}(\text{NHC})_2$ is in the catalytic cycle. This possibility has been tested by numerical integration after steady-state approximations for $[\text{Pd}(\text{NHC})]$ and $[\text{Pd}(\text{NHC})(\text{Ar})(\text{X})]$ are made. This model gives $k_3 \approx 2.4 \times 10^{-4} \text{ M}^{-1} \text{ s}^{-1}$, but requires that $k_1 \approx 2.8 \times 10^{-4} \text{ s}^{-1}$, which is 40 times larger than the value from the stoichiometric study. Therefore, this does not appear to be a viable alternative.

Conclusions

The overall picture that emerges from this analysis is that the relationship between the stoichiometric oxidative addition and the catalytic amination kinetics is more complex than it would appear from the published analyses. Unfortunately, the direction and magnitude of the discrepancies are variable so that it is difficult to draw general conclusions about the source(s) of the problems.

The calculated rate constants for the catalytic study of the $\text{Pd}(\text{BINAP})_2$ -PhBr-hexylamine system (see Figure 2) are much larger than those observed unless one ignores the k_4 pathway, but for the 2 M PhBr of the catalytic study, the k_4 pathway is dominant on the basis of the stoichiometric kinetics (see Figure 1). On the other hand, a study of the same reaction with different reagent concentrations and in a different laboratory found the rate to be about 6 times larger than would be predicted by the stoichiometric rate constants, even with the k_4 pathway included. In the case of 3-bromoanisole, where the stoichiometric reaction and the catalytic reaction with *N*-methylpiperazine seem to have been done by the same experimenter, the calculated catalytic rate is just 1.5 times smaller than predicted, as shown in Figure 4.

One feature that has received little attention here or in the published work is the effect of the $\text{Pd}(0)$ concentration. The stoichiometric studies typically have used $(3 - 5) \times 10^{-5} \text{ M}$ $\text{Pd}(\text{BINAP})_2$, while the catalytic studies were in the $(1 - 10) \times 10^{-3} \text{ M}$ range. It is generally assumed, but not demonstrated, that the catalytic rate is first-order in total Pd.

It should be noted that Blackmond and co-workers⁴ recently have found rather different kinetics for the coupling of a phenyl hydrazone with 3-(F_3C) $\text{C}_6\text{H}_4\text{Br}$ at 90 °C in toluene using Pd-

(OAc)₂ and BINAP as the precatalyst.²³ The rate has a zeroth-order dependence on [hydrazone], and what is really different is the rate also is zeroth-order in [ArBr]. Blackmond and co-workers suggested that the "resting state" for this system is a $\text{Pd}^{\text{II}}(\text{Ar})(\text{hydrazone})$ species. To accommodate this proposal, the mechanism in Scheme 1 must be modified by including $\text{PdL}(\text{Ar})(\text{NH}_2\text{R})$ as the product of the k_3 step and adding its reductive elimination by k_5 . Numerical modeling of the results of Blackmond and co-workers is somewhat speculative because the Pd or BINAP concentrations were not reported. However, reasonable assumptions²⁴ show that the kinetic behavior is predicted with $k_1 \approx 0.015 \text{ s}^{-1}$ and $k_5 \approx 0.08 \text{ s}^{-1}$. With due allowance for the differences in temperature and possibly the catalyst, these values are reasonably consistent with the values of k_1 in Table 1 and of k_5 determined by Hartwig²⁵ for $\text{Pd}(\text{DPPF})(p\text{-MeOC}_6\text{H}_4)(\text{NHNCPh}_2)$ at 70 °C in toluene. Calculated and experimental results are given in the Supporting Information, where it is also shown that $\text{PdL}(\text{Ar})(\text{NHNCPh}_2)$ is a significant Pd species during the course of the reaction.

It would appear that the phenyl hydrazone system is kinetically different from the various amines that have been studied under catalytic conditions because the reductive elimination is much slower. Hartwig found that reductive elimination from the diphenyl hydrazone system mentioned above with $\text{Ar} = p\text{-MeOC}_6\text{H}_4$ has $k_5 = 3.8 \times 10^{-4}$ (70 °C), while Driver and Hartwig²⁶ reported $k_5 = 2.1 \times 10^{-4}$ (75 °C) with $\text{N}(p\text{-tolyl})_2$ and the same Ar. From these data it would appear that the reactivity of the hydrazone is similar to that of a diarylamine. In the same study it was observed that the reactivity order is $\text{NHR} > \text{NHPh} > \text{NPh}_2$, and the effect has been attributed²⁷ to the decreasing basicity of the N-center. Since the other catalytic studies have involved the much more reactive primary or secondary aliphatic amines (hexylamine, piperazine, morpholine), it is understandable that reductive elimination has not been a rate-limiting feature.

The analysis of the $\text{Pd}(\text{NHC})_2$ system under catalytic conditions has unraveled the complexities of the second-order experimental conditions. For the one set of conditions used, the catalytic rate is consistent with the stoichiometric results if one assumes that the substitution of chloride by amine has some kinetic influence.

Acknowledgment. I thank the University of Alberta for financial support of this work.

Supporting Information Available: Text and figures giving details of the steady-state conditions and numerical integration, kinetic analysis of the system in ref 5, and Figures S1–S3. This information is available free of charge via the Internet at <http://pubs.acs.org>.

OM7003223

(23) The nature of the catalytic species formed from these reagents was studied by Wolfe and Buchwald: Wolfe, J. P.; Buchwald, S. L. *J. Org. Chem.* **2000**, *65*, 1144.

(24) The calculations assume that the total Pd is 5 mM as in ref 25 and there is no excess BINAP.

(25) Hartwig, J. F. *Angew. Chem., Int. Ed.* **1998**, *37*, 2092.

(26) Driver, M. S.; Hartwig, J. F. *J. Am. Chem. Soc.* **1997**, *119*, 8232.

(27) Hartwig, J. F. *Inorg. Chem.* **2007**, *46*, 1936.